Plio-Quaternary exhumation history of the central Nepalese Himalaya: 1. Apatite and zircon fission track and apatite [U-Th]/He analyses

A. E. Blythe,[1,2] D. W. Burbank,[3] A. Carter,[4] K. Schmidt,[5] and J. Putkonen[6]

Received 5 May 2006; revised 19 October 2006; accepted 22 December 2006; published 4 May 2007.

[1] New apatite and zircon fission track and (U-Th)/He analyses serve to document the bedrock cooling history of the central Nepalese Himalaya near the Annapurna Range. We have obtained 82 apatite fission track (AFT), 7 zircon fission track (ZFT), and 7 apatite (U-Th)/He (AHe) ages from samples collected along the Marsyandi drainage, including eight vertical relief profiles from ridges on either side of the river averaging more than 2 km in elevation range. In addition, three profiles were sampled along ridge crests that also lie ~2 km above the adjacent valleys, and a transect of >20 valley bottom samples spans from the Lesser Himalaya across the Greater Himalaya and into the Tethyan strata. As a consequence, these data provide one of the more comprehensive low-temperature thermochronologic studies within the Himalaya. Conversely, the youthfulness of this orogen is pushing the limits of these dating techniques. AFT ages range from >3.8 to 0 Ma, ZFT ages from 1.9 to 0.8 Ma, and AHe ages from 0.9 to 0.3 Ma. Most ridges have maximum ages of 1.3–0.8 Ma at 2 km above the valley bottom. Only one ridge crest (in the south central zone of the field area) yielded significantly older ZFT and AFT ages of ~2 Ma; we infer that a splay of the Main Central Thrust separates this ridge from the rest of the Greater Himalaya. ZFT and AFT ages from a vertical transect along this ridge indicate exhumation rates of ~1.5 km Myr^{-1} ($r^2 > 0.7$) from ~2 to 0.6–0.8 Ma, whereas AHe ages indicate a faster exhumation rate of ~2.6 km Myr^{-1} ($r^2 = 0.9$) over the last 0.8 Myr. Exhumation rates calculated for six of the remaining seven vertical profiles ranged from 1.5 to 12 km Myr^{-1} (all with low r^2 values of <0.6) for the time period from ~1.2 to 0.3 Ma, with no discernible patterns in south to north exhumation rates evident. The absence of a trend in exhumation rates, despite a strong spatial gradient in rainfall, argues against a correlation of long-term exhumation rates with modern patterns of rainfall. AFT ages in the Tethyan strata are, on average, older than in the Greater Himalaya and may be a response to a drier climate, slip on the South Tibetan Detachment, or a gentler dip of the underlying thrust ramp. These data are further evaluated with thermokinematic modeling in the companion paper by Whipp et al. **Citation:** Blythe, A. E., D. W. Burbank, A. Carter, K. Schmidt, and J. Putkonen (2007), Plio-Quaternary exhumation history of the central Nepalese Himalaya: 1. Apatite and zircon fission track and apatite [U-Th]/He analyses, *Tectonics*, *26*, TC3002, doi:10.1029/2006TC001990.

1. Introduction

[2] Theoretical controls on exhumation rates by climate variations and their possible effects on tectonic processes [*Molnar and England*, 1990; *Willett*, 1999; *Beaumont et al.*, 2001] have led to recent field studies searching for potential linkages of climate with tectonics. Apparent correlations of spatial variations in exhumation rates with variations in precipitation suggest a causal relationship [*Dadson et al.*, 2003; *Reiners et al.*, 2003; *Thiede et al.*, 2004, 2005], but the debate over whether or not increased precipitation rates do affect the location of active faulting remains to be resolved. Given an intense summer monsoon, spectacular topographic variations, and rapid tectonic deformation, the Himalaya represent an obvious field site in which to address this question.

[3] In this study, we document the cooling and exhumation history of the Himalaya in central Nepal, along the Marsyandi drainage, with a large suite of apatite fission track, zircon fission track and (U-Th)/He analyses. These thermochronologic data are being used with geomorphic and climate data to evaluate the mechanisms controlling the physiography of the Nepal Himalaya. In the companion paper that follows [*Whipp et al.*, 2007], the apatite fission track analyses from this study are further evaluated with thermokinematic modeling. The question we are ultimately interested in is whether or not climate exerts key controls on rates of exhumation and on the locus of major deformation in the Himalaya. The Indian Monsoon focuses its most intense rainfall on the outer, southern margin of the Lesser Himalaya and on the southern slopes of the Greater

[1]Department of Earth Sciences, University of Southern California, Los Angeles, California, USA.
[2]Now at Geology Department, Occidental College, Los Angeles, California, USA.
[3]Department of Earth Science, University of California, Santa Barbara, California, USA.
[4]School of Earth Sciences, Birbeck College, University of London, London, UK.
[5]Department of Natural Sciences, Lewis-Clark State College, Lewiston, Idaho, USA.
[6]Department of Earth and Planetary Science, University of Washington, Seattle, Washington, USA.

0278-7407/07/2006TC001990

Himalaya between altitudes of 2–3 km [*Barros and Lang*, 2003; *Bookhagen et al.*, 2004; *Bookhagen and Burbank*, 2006]. Monsoon rainfall diminishes to the north, such that across the Greater Himalaya (~25 km), summer precipitation decreases about tenfold (Figure 1). If climate modulates exhumation rates, then cooling ages that span this tenfold precipitation gradient should reveal pronounced differences in reconstructed exhumation rates. Exhumation rates and rainfall distributions appear uncorrelated in the data presented here and therefore suggest that modern rainfall patterns may not be suitable predictors of variations in long-term exhumation rates.

2. Geologic Setting

[4] Since the collision of India with southern Asia began at ~50 Ma [*Rowley*, 1996], more than 2600 ± 900 km of Indo-Asian convergence has occurred [*Besse and Courtillot*, 1988], creating the Himalaya and the Tibetan Plateau. Successive underthrusting and accretion of Indian crust to Asia has created an orogenic wedge that extends south of the Indus suture and underlies the present-day Himalaya. The major south vergent thrust faults within the Himalaya generally get younger toward the south. The Main Central Thrust (MCT,) which forms the southern boundary of the Greater Himalaya, was active from late Oligocene until early Miocene [*Hodges*, 2000; *Searle and Godin*, 2003]. Farther south, the Main Boundary Thrust (MBT) initiated at 10–12 Ma [*Meigs et al.*, 1995] and carries the Lesser Himalaya over the Himalayan foreland. Within the foreland, the southernmost active thrust is the Main Frontal Thrust of Plio-Pleistocene age [*Lavé and Avouac*, 2000]. On the northern edge of the Greater Himalaya, the South Tibetan Detachment (STD) fault system, a suite of down-to-the-north normal faults that separates the Greater Himalayan rocks from the Tethyan strata of southern Tibet [*Hodges*, 2000], was active during the early Miocene [*Searle and Godin*, 2003]. The STD, MCT, and MBT can be traced nearly across the entire length of the Himalayan arc and demonstrate a remarkable coherence of deformation over the past 25 Myr.

[5] This study is focused in the Marsyandi catchment that spans from the southern Tibetan Plateau to the Himalayan foreland in central Nepal. The catchment encompasses all of the major Himalayan lithotectonic units, including the >8-km-high Manaslu and Annapurna ranges. Despite more than 3 decades of geologic mapping, the position of some of the major faults within the study area is still debated. *Searle and Godin* [2003] define the South Tibetan Detachment as equivalent to their Phu detachment fault (Figure 2), and they interpret the more southerly Chame detachment as an extensional fault within the Greater Himalaya. On the basis of offset $^{40}Ar/^{39}Ar$ cooling ages across the Chame detachment fault [*Coleman and Hodges*, 1998] and the presence of the Annapurna Yellow Formation in its hanging wall, we consider the Chame detachment as equivalent to the South Tibetan Detachment in our study area. Following *Coleman* [1996], we interpret the more northerly Phu detachment [*Searle and Godin*, 2003] as a younger extensional fault that cuts both Tethyan strata and the Manaslu granite in the hanging wall of the Chame detachment. The position of the Main Central Thrust is also debated in our study area. *Hodges et al.* [2004] mapped multiple thrusts in the footwall of the traditional location of the MCT at the base of Formation I gneisses [*Colchen et al.*, 1986]. *Martin et al.* [2005] argue for a more southerly position of the MCT with respect to its traditional location. For our purposes, samples we assign to the footwall of the MCT lie south of the fault interpreted as the MCT in each of these studies. Until recently, the prevailing consensus was that after the MBT formed, deformation ceased along the MCT. Several studies in the past decade have suggested deformation in the footwall of the Main Central Thrust of either latest Miocene-to-Pliocene [*Harrison et al.* 1997; *Catlos et al.*, 2001] or Quaternary [*Hodges et al.*, 2004; *Wobus et al.*, 2003, 2005; *Huntington and Hodges*, 2006] age. Although the cause of this out-of-sequence deformation remains unknown, focused deformation in response to intense monsoonal rainfall has been suggested [*Hodges et al.*, 2004].

[6] The present study utilizes samples collected within the Marsyandi catchment in the central Nepalese Himalaya. There have been numerous previous low-temperature thermochronology studies in the Himalaya. Apatite FT ages from comparable structural locations elsewhere in the Himalaya have ranged from <1 to 4 Ma in Nanga Parbat [*Zeitler et al.*, 1985], Bhutan [*Grujic et al.*, 2006], and northwestern India [*Thiede et al.*, 2004, 2005]. The youngest Himalayan ages (zircon and apatite FT ages of $\leq$1 and 0.5 Ma, respectively) have come from the Namche Barwa syntaxis [*Burg et al.*, 1997; *Seward et al.*, 2004]. *Bojar et al.* [2005] obtained a similar suite of sample ages (apatite and zircon FT and He analyses) from a structurally similar location in the Goriganga valley of the central Himalaya (to the west of our study). The geographically closest previous study to our field area comprises zircon FT analyses from the Kali Gandaki (the major drainage to the west of the Marsyandi) with ages ranging from 2.5 to 1.0 Ma [*Arita and Ganzawa*, 1997]. In the present study, we obtain apatite fission track ages comparable to those from Namche Barwa and the Goriganga valley, and zircon ages that are similar to those from the Kali Gandaki.

[7] *Huntington et al.* [2006] previously used muscovite $^{40}Ar/^{39}Ar$ ages and a subset of the apatite fission track ages discussed here from Nagi Lek, a ridge in the southeastern part of the study area, to document a striking increase in apparent exhumation rate between 2.5 and 0.9 Myr, which they attributed to a change in climate. In this study, we use fission track and (U-Th)/He analyses to examine the apparent exhumation rate in the time period from ~2 to 0.3 Myr.

3. Methodology

[8] Fission tracks are linear zones of damage in the crystal lattice that form as the result of the spontaneous fission of ^{238}U. The tracks are unstable at higher temperatures: the crystal lattice heals itself as the fission tracks

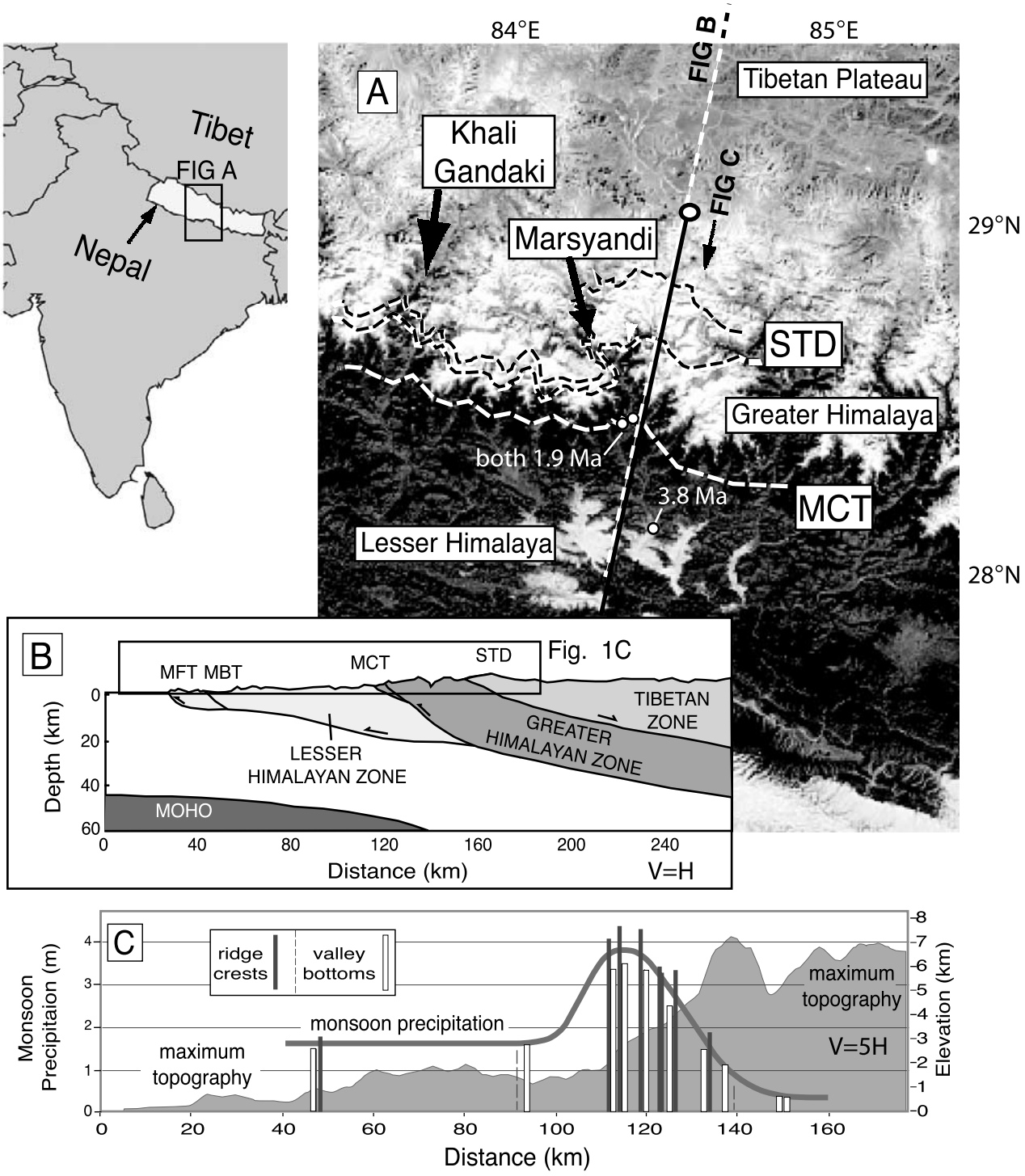

Figure 1. Regional map (top left) showning the location of the study area. (a) Satellite image in the central Nepalese Himalaya with major drainages and geologic regions and structures. The white dashed line shows the general location of the Main Central Thrust (MCT). The black dashed lines show the possible locations of the South Tibetan Detachment (STD). Apatite fission track ages for three samples south of the MCT are shown. See text for further discussion. (b) Generalized cross section (location shown on Figure 1a, which extends beyond the satellite image to the north and south) of the central Nepal Himalaya, showing locations of major faults [after *Hodges et al.*, 2001]. (c) Profile of maximum topography with mean monsoon precipitation [after *Burbank et al.*, 2003]. Location of profile is shown on Figure 1a, extending southward beyond the satellite image.

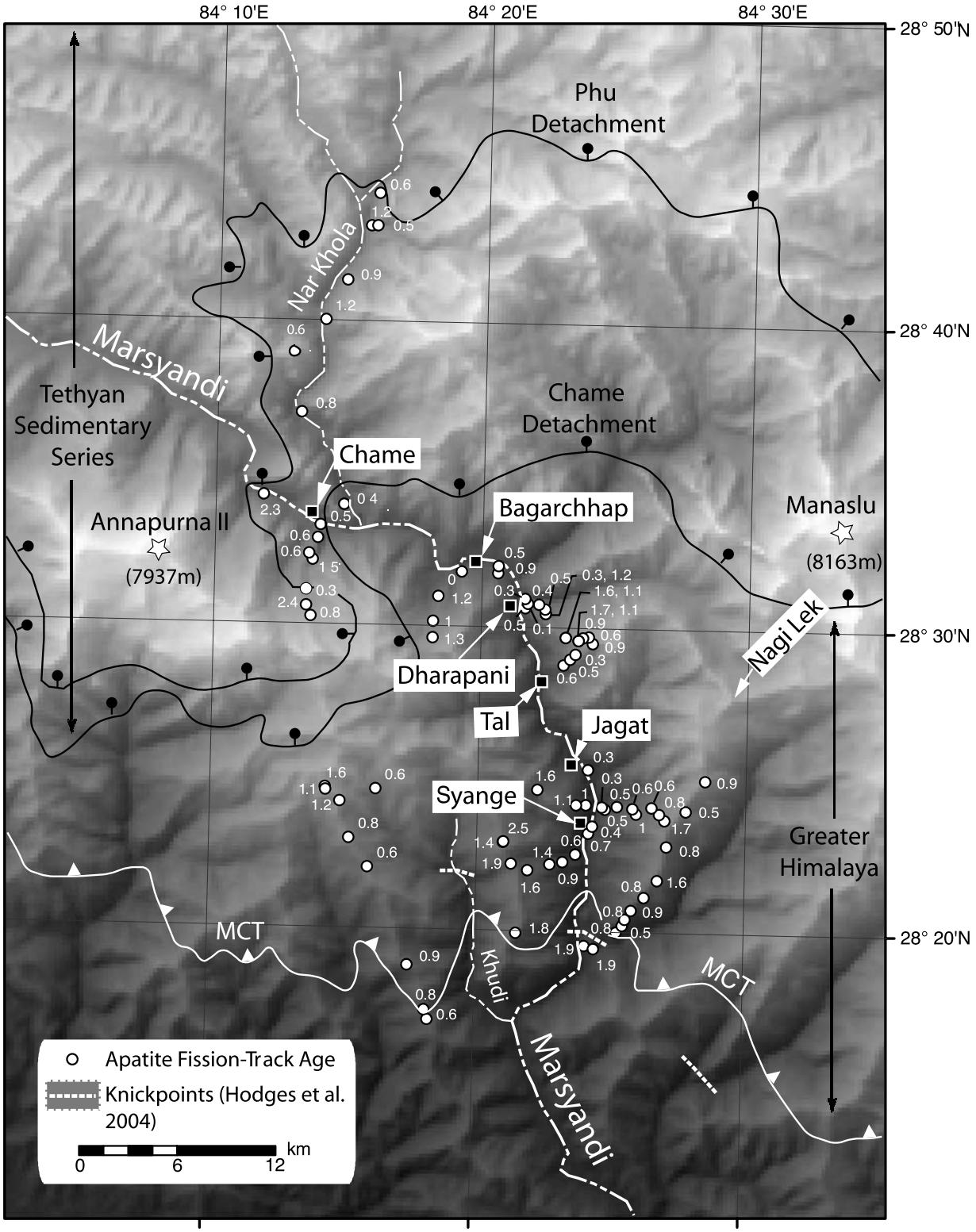

Figure 2a. Digital elevation model of the Marsyandi drainage, central Nepal. Sample locations and ages (in million years) are shown, as well as recently mapped locations of the Chame and Phu detachment faults [*Coleman and Hodges*, 1998; *Searle and Godin*, 2003] and the Main Central Thrust (MCT) [*Hodges et al.*, 2004]. Dashed lines show the locations of recently recognized knickpoints [*Hodges et al.*, 2004], which are discussed in the text.

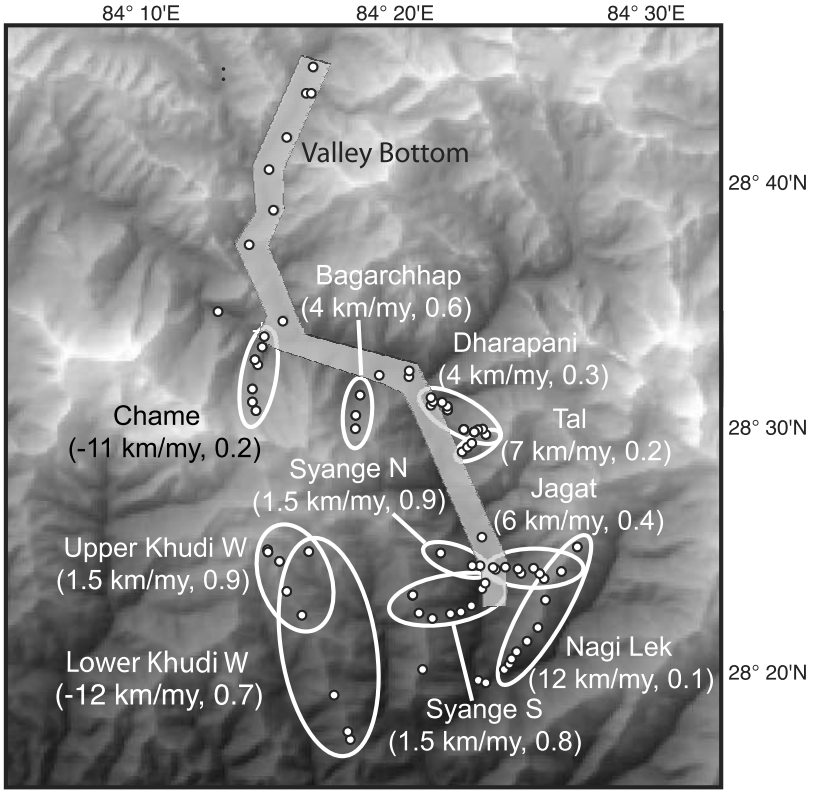

Figure 2b. Locations for sample transects, along with the exhumation rate calculated for each transect, followed by the r^2 value for the exhumation rate calculation.

anneal. Annealing occurs over a range of temperatures, with slower annealing at lower temperatures. The range of temperatures over which annealing occurs is called the "partial annealing zone" [e.g., *Gleadow and Fitzgerald*, 1987]. At moderate geologic cooling rates ($\sim$10°C Myr^{-1}), track annealing is sufficiently slow for tracks to be retained in low-chlorine apatites at $\leq$110°C and are relatively stable by $\sim$60°C [*Green et al.*, 1986; *Ketcham et al.*, 1999]. In zircons, for the same cooling rate, tracks begin to accumulate at $\sim$350 to 250°C [*Tagami and Dumitru*, 1996; *Tagami et al.*, 1996, 1998; *Rahn et al.*, 2004]. At faster cooling rates (100°C Myr^{-1}), tracks are preserved in the crystal lattice at higher temperatures of $\sim$140 to 170°C for apatite and $\sim$330 to 250°C for zircon [*Ketcham et al.*, 1999; *Tagami and Dumitru*, 1996; *Tagami et al.*, 1996, 1998; *Rahn et al.*, 2004]. In (U-Th)/He thermochronometry, which is based on the release of He during the decay of U and Th, He begins to accumulate in the crystal lattice of apatite at 70–75°C for average geologic cooling rates [*Farley*, 2000]. At cooling rates of 100°C Myr^{-1}, He retention begins to occur at $\sim$90°C in apatite [*Farley*, 2000].

[9] Thermochronometric data, such as apatite and zircon fission track and (U-Th)/He analyses, are commonly used to evaluate the low-temperature cooling history of regions. With these data, exhumational histories are calculated in at least two ways. In the first, the sample age (A), which represents the time since cooling through a known closure temperature [*Dodson*, 1973], T_c, is used with an assumed geothermal gradient (dT/dz) to calculate an exhumation rate, E_r:

$$E_r = [(T_c - T_s)/A]/(dT/dz),$$

where T_s equals the average temperature at the surface. For estimating exhumation rates with fission track ages, this approach should only be used if cooling is rapid. The second approach uses elevation transects, in which samples are collected at different elevations from a borehole or vertical cliff [*Fitzgerald and Gleadow*, 1988], with the samples recording the passage through progressively lower temperatures as rock is exhumed along a vertical pathway to the surface. The vertical gradient of ages reflects exhumation rates that may be constant or changing through time. This approach also assumes a topographic steady state [*Burbank and Anderson*, 2001; *Willett and Brandon*, 2002], such that vertical changes in the position of the closure temperature occur as a direct response to average surface lowering, rather than to transient changes in relief. In reality, topographic steady state is untestable, at least directly. Moreover, truly vertical relief sections are rare, at least over the distances required to record statistically significant variations in cooling rate. Hence samples are often collected along steep and extensive topographic transects. In this study, we use both approaches to try to estimate exhumation rates: we collected bedrock samples at river level and from several transects along ridges rising nearly

perpendicular to the river. These latter are referred to as vertical transects, and although the data are plotted on age versus elevation plots, none of these samples were collected on truly vertical cliffs, and therefore care must be used in interpreting the data. Many of these transects are steep, however, rising >2 km in <5 km horizontal distance.

4. Thermochronometry Results

[10] A total of 82 apatite and 7 zircon fission track and 7 apatite (U-Th)/He ages have been obtained from samples collected within the Marsyandi drainage basin (Figure 2 and auxiliary material Tables S1, S2, and S3, respectively).[1] The apatite fission track analyses presented here are unusually young, reflecting the rapidity of the processes they document: apatite fission track ages range from 0.0 ± 0.4 Ma to 3.8 ± 1.0 Ma (reported errors are two sigma). The zircon fission track ages, which ranged from 1.9 ± 0.4 to 0.8 ± 0.2 Ma, and the (U-Th)/He ages of 0.88 ± 0.04 to 0.3 ± 0.02 Ma.

[11] In order to reduce bias in the fission track analyses, all but 13 of the apatite fission track samples were analyzed without the analyst (Blythe) being aware of the sample's location (the remaining 13 samples were collected by Blythe). On the Dharapani transect (Figure 2b), a pair of samples, one host rock and the other pegmatite, was collected from three different locations (pegmatite samples are designated by "p" in Table S1). The paired ages of the pegmatite and host rock can be quite different; in the worst case, the host rock yielded an age of 0.3 ± 0.2 and the pegmatite an age of 1.2 ± 1.0 Ma. Although these ages overlap at the 2-sigma level, they illustrate the importance of considering errors in fission track analyses. Errors on the ages are primarily a function of the amount of U in each sample and the total number of grains analyzed (shown in Table S1).

[12] Exhumation rates (Figure 2 and auxiliary material Table S4) were derived by, first, creating error-weighted, least squares linear regressions of the elevation versus cooling age data using Isoplot [*Ludwig*, 2003], such that ages with larger errors affected the exhumation rates less than ages with smaller errors. Because the elevation is well defined, the cooling age is the dependent variable. This regression result was then inverted to yield an elevation/age ratio that can be interpreted as an exhumation rate. The data are presented in the traditional format of age versus elevation and include the inverted regression line. Given the 95% confidence interval on these inverted slopes, these regressions yield negative exhumation rates for some transects: we interpret these as "infinite" rates. The exhumation rate calculations are summarized in Table S4 in the auxiliary material.

[13] As is typical with many such estimates of exhumation rates from relief transects [e.g., *Fitzgerald et al.*, 1995; *Brewer et al.*, 2003; *Huntington and Hodges*, 2006], these calculations utilize three key assumptions: (1) vertical particle paths toward the surface, (2) horizontal closure isotherms, with elevation directly proportional to the depth of the isotherm, and (3) valley cutting is not considered to be significant (valley cutting could yield variable exhumation rates at shallow depths [e.g., *van der Beek et al.*, 2002]). Although none of these are strictly true in the Himalaya, the straightforward calculations of exhumation rates based on them should provide insights into spatial variations along a broad transect across the Himalaya. One of the difficulties in evaluating these data sets is deciding whether age variations are the result of thermal changes, analytical problems, structural features (previously recognized or unrecognized), or a genuine change in exhumation rate. We discuss these possibilities as we analyze the data sets.

4.1. River Level Samples

[14] Initially, we examine those samples that were collected within a 200-m elevation range of the Marsyandi and Nar river valley bottoms and that represent a transect approximately perpendicular to the range axis. This 24-sample transect extends from 500 m elevation in the Lesser Himalaya to 4000 m in the Tethyan strata and, in its southern part, the transect crosses the Main Central Thrust (Figure 3). The transect subsequently crosses the Chame detachment (the main expression of the South Tibetan Detachment in this area [*Coleman and Hodges*, 1998]) and ends just south of the Phu Detachment (Figures 1 and 2). The suite of Greater Himalayan samples south of the Chame Detachment (~28.6°N latitude) have been previously interpreted to indicate uniformly rapid exhumation within the Greater Himalaya [*Burbank et al.*, 2003].

[15] The southernmost sample, with an apatite fission track age of 3.8 ± 1.0 Ma, from the Lesser Himalaya ~35 km south of the Main Central Thrust, is significantly older than any other sample (this sample location is not shown on Figure 2a, all other sample locations are shown). The next two samples to the north along the Marsyandi both yielded ages of 1.9 ± 2.2 Ma; these samples lie in the proximal footwall of the MCT, <2–3 km from the fault. The remaining river level samples are from the Greater Himalaya, and Tethyan strata, and range in age from 0.0 ± 0.4 to 2.3 ± 3.2 Ma. Two general observations emerge from these data (Figure 3). First, throughout the transect north of the MCT, the cooling ages are young: all but three are <1 Ma. The mean AFT age for the entire Greater Himalayan-Tethyan transect is 0.6 Ma (n = 19) which yields an average cooling rate of >200°C Myr^{-1}, assuming tracks began to accumulate at ≤140°C, the assumed closure temperature for fission tracks in apatite under very rapid cooling conditions [see *Ketcham et al.*, 1999]. Second, when viewed as a whole, there appears to be a slight, northward rising trend in age, although the trend has a low statistical significance (r^2 = 0.23) and actually contains two other weak trends: within the Greater Himalaya, ages trend younger toward the north, while within the Tethyan rocks, ages show no spatial trend.

[16] Interpretation of the overall trend is complicated by the increase in elevation from south to north along the river: older ages are generally expected at higher elevation over

[1] Auxiliary materials are available at ftp://ftp.agu.org/apend/tc/2006tc001990.

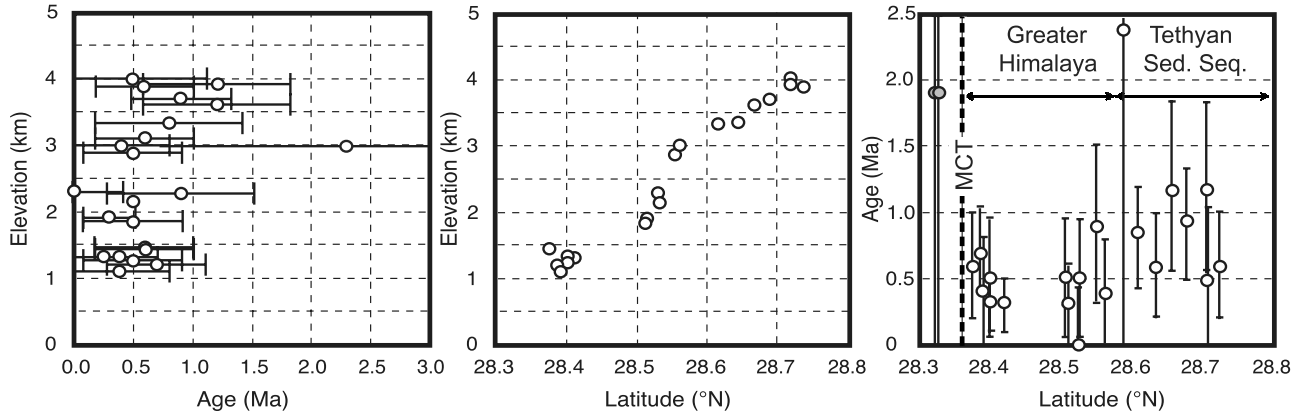

Figure 3. (left) Apatite fission track ages plotted with respect to elevation for the valley bottom samples collected to the north of the Main Central Thrust (MCT) along the Marsyandi and Nar Khola. (middle) Elevation of the same valley bottom samples plotted relative to latitude. (right) Apatite fission track ages plotted relative to latitude.

short distances. These samples, however, were collected along the river channel over >40 km of N-S distance. It is therefore reasonable to assume that the depth of the closure isotherm beneath the N-S transect paralleled the rise in sample elevation (Figure 3, middle). On average, valley bottom ages in the Tethyan rocks are ~0.36 Myr older than those in the Greater Himalaya, although even in the far northern parts of the transect, some cooling ages are as young as those just north of the MCT (Figure 3, right). Given that monsoon rainfall decreases about tenfold across this same region, it could be interpreted that exhumation rates decrease as it becomes drier. On the other hand, evidence from the northern flank of the Annapurna Range and Thakkhola Graben suggests that the South Tibetan Detachment fault system has been reactivated during the Quaternary [*Hurtado et al.*, 2001]. Down-to-the-north slip on the Chame Detachment might explain the older ages and their implications for slower exhumation in the Tethyan strata in its hanging wall (Figure 3).

[17] Within the Greater Himalaya, the apatite fission track ages either become younger toward the north or remain constant (Figure 3, right). From south to north across this same terrain, monsoonal rainfall decreases by greater than or equal to fourfold (Figure 1). Comparison of these spatial data sets suggests that the pattern of exhumation at Quaternary timescales does not correlate with the distribution of modern rainfall [*Burbank et al.*, 2003].

4.2. Strike-Parallel and -Perpendicular Transects

[18] The remaining fission track samples are divided into two categories: strike-parallel and strike-perpendicular. The former group comprises more typical "vertical relief sections." We distinguish between these groups because rocks along transects in these orientations can have rather different relationships to the three-dimensional surface defined by the reference isotherm of 140°C (see Figure 4). The more spread out the samples are in terms of where they crossed the 140°C isotherm, the greater the uncertainty in relative and absolute distance traveled between the isotherm and the surface. When samples were derived from a broad latitudinal span along that isotherm, it becomes more difficult to discern whether an older age indicates a slower exhumation rate or

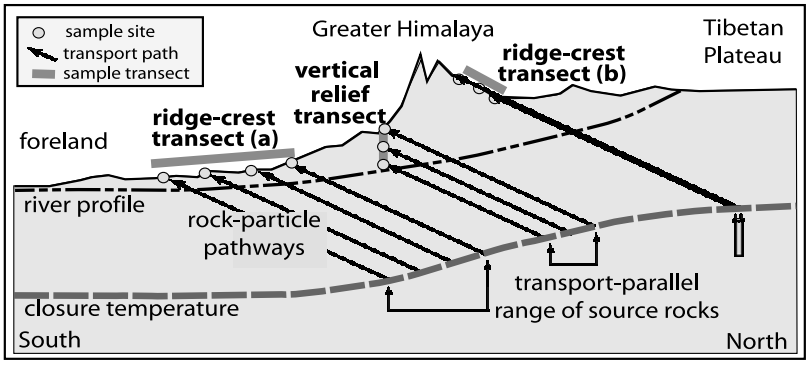

Figure 4. Schematic diagram of transect orientation versus particle path toward closure isotherms, comparing the particle pathways for vertical relief transects and ridge crest transects. See text for further discussion.

simply a longer distance between the isotherm and the surface.

[19] The vertical relief transects were collected approximately parallel to strike and perpendicular to both the Marsyandi valley and the orogenic transport direction. These transects typically begin at or near river level, and ascend steeply (21°–34°) over horizontal distances of 3–6 km to elevations ~2 km above nearby valley bottoms. Whereas such geometries are considered optimal for calculating exhumation rates in orogens in which rock particles move vertically toward the surface, lateral advection in the Himalaya dictates that particle pathways for these rocks are moderately separated along the closure isotherm (Figure 4). The Tal, Jagat, Syange, and Dharapani sections are classified as vertical-relief, strike-parallel transects here (Figure 2b).

[20] In the second grouping, samples were collected along ridgelines and slopes that trend nearly perpendicular to the strike of the range and are parallel to both the central reaches of the Marsyandi River and the overall, regional tectonic transport direction of overthrusting [*Searle and Godin*, 2003; *Wang et al.*, 2001]. These transects can be further subdivided into longer transects that lie along ridges that generally slope gently to the south (mean ~10°) and shorter transects along ridges that dip more steeply to the north (~20°). These contrasting orientations dictate that successive samples along a ridge have fundamentally different spatial relationships to each other in terms of thermal history (Figure 4). For example, the 20° north dipping ridges are almost parallel to the foliation and the inferred rock transport direction above a deep-seated ramp [*Pandey et al.*, 1995; *Seeber et al.*, 1981; *Brewer and Burbank*, 2006]. Hence samples along each such transect (e.g., the Bagarchhap and Chame sections) could, in theory, follow a single particle pathway to the surface (transect b, Figure 4). In contrast, the gently south dipping ridges yield samples that come from a broader latitudinal spread of positions along the closure isotherm (transect a, Figure 4). Such transects include the Khudi ridges and Nagi Lek (Figure 2b).

4.2.1. Strike-Parallel Transects

[21] The samples in these transects derive from a limited latitudinal range (Figure 4) and are treated as if they had a common pathway toward the surface. Hence we analyze them as vertical relief transects.

4.2.1.1. Jagat

[22] In the southern Greater Himalaya, the Jagat transect comprises nine samples that begin at the Marsyandi River near the village of Jagat and span 2.6 km of elevation over a horizontal distance of ~5 km (Figure 2b). The mean topographic slope of the transect is 27°. The lowest samples are ≤0.5 Ma and, although the samples tend to get older with higher elevation, the highest sample also yielded an age of 0.5 Ma (Figure 5a). When younger ages are superposed above older ones, this could suggest the presence of a thrust fault separating the different aged samples. The uncertainties with these ages are sufficiently large that this possibility cannot be evaluated: Hence we make no structural interpretation. Overall, these data from Jagat indicate a mean exhumation rate of $5.7^{+\mathrm{inf}}_{-2.9}$ km Myr^{-1} ($r^2 = 0.38$). The relatively low r^2 values (also seen in most other transects) are not unexpected given the large uncertainties associated with these ages (Table S1 and Figure 5a).

4.2.1.2. Dharapani

[23] The relief transect with the largest number of samples came from a single ridgeline to the east of the village of Dharapani (Figure 2b). The transect spans 2900 m of elevation across a distance of ~5 km with a mean topographic slope of 30°. In three locations, samples were collected from pegmatites, as well as the adjacent host rocks. The exhumation rate (Figure 5b) derived from all of the Dharapani samples (including both pegmatite and host samples) is $3.8^{+2.8}_{-1.8}$ km Myr^{-1} ($r^2 = 0.33$).

4.2.1.3. Tal

[24] The Tal relief section (Figure 2b) is abbreviated, encompassing only four samples and spanning 1.7 km of elevation across a distance of 2.5 km with a mean topographic slope of 34°. The topmost sample is shared with the Dharapani transect. Overall, this transect is oriented NE-SW, so that it rises obliquely across strike. All ages in the transect are <1 Ma, and, neglecting errors, the middle two ages are younger than the lowest age. These data yield a mean exhumation rate (Figure 5c) of $6.7^{+\mathrm{inf}}_{-5.2}$ km Myr^{-1} ($r^2 = 0.20$).

4.2.1.4. Syange South

[25] The Syange South transect is located in the southwestern part of the field area, progressing up the ridge to the west of the village of Syange (Figure 2b). Eight samples were collected along this ridgeline at elevations ranging from 1210 to 3100 m. From these samples, we obtained eight apatite and five zircon fission track and six apatite (U-Th)/He analyses (Figure 6a). Apatite fission track ages range from 0.6 ± 0.4 to 2.5 ± 1.0 Ma. Zircon fission track ages range from 0.8 ± 0.2 to 1.9 ± 0.4 Ma and are within one sigma of the apatite fission track ages, although two apatite ages are slightly older than the zircon ages from the same samples. Apatite (U-Th)/He ages from many of these same samples were younger, ranging from 0.9 to 0.3 Ma. All of these analyses reveal rather linear age versus elevation relationship (r^2 values of ≥0.74). Error-weighted exhumation rates are $1.4^{+6.3}_{-0.6}$, $1.5^{+1.2}_{-0.5}$ and $2.6^{+2.9}_{-0.9}$ km Myr^{-1} for the zircon fission track, apatite fission track, and apatite He ages, respectively. The time periods covered by the zircon and apatite fission track data overlap from ~2 to 0.7 Ma, whereas the He data covers a younger time period, from ~0.9 to 0.3 Ma. These data suggest an increase in exhumation rate at ~0.8 Myr, although compression of isotherms toward the surface in rapidly eroding terrains could explain some of the apparent acceleration in rates. Evaluation of these data with thermokinematic modeling is used to further test this suggestion by *Whipp et al.* [2007].

[26] Although these data yield rather linear age-elevation relationships that suggest the exhumation rates calculated from them should be reliable, two intriguing contradictions lie within these data. First, the zircon fission track ages are on average, only slightly older than the apatite ages from the exact same sample. Given the differences in assumed closure temperatures (330°–250° versus 140°C) for zircon and apatite, their age differences imply cooling at rates >500°C Myr^{-1} between the time of closure for the zircons and apatites. Such a high cooling rate is incompatible with

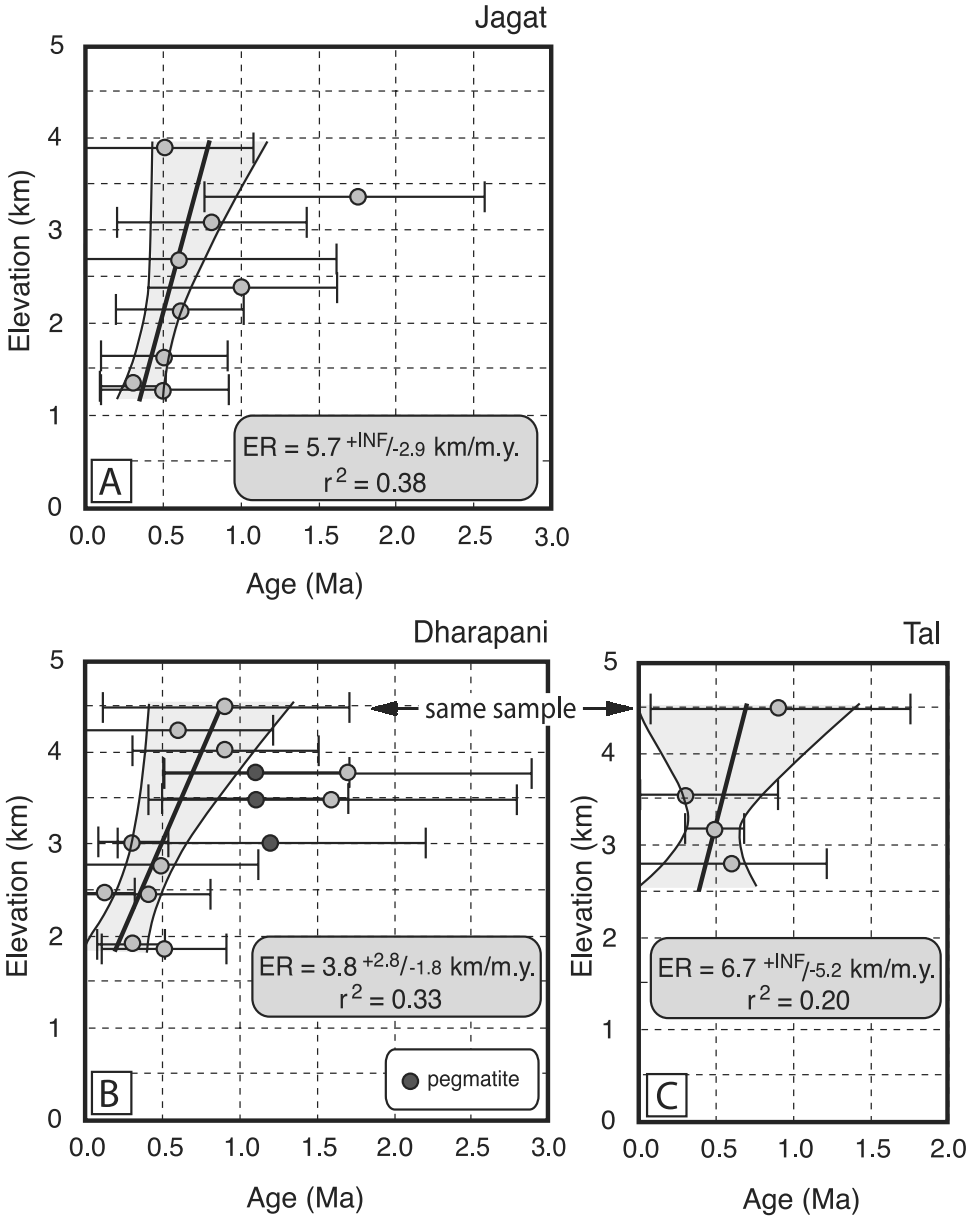

Figure 5. Apatite fission track ages plotted against sample elevations for samples collected on three vertical relief transects: (a) Jagat, (b) Dharapani, and (c) Tal. Lines define mean exhumation rates calculated using an error-weighted least squares linear regression; 95% confidence intervals are shown. Note that the uppermost sample is the same for the Dharapani and Tal transects and that the Dharapani transect includes three sets of paired (bedrock and pegmatite) samples. See Figure 2b for transect locations and the text for further discussion.

an exhumation rate of 1.5 km Myr^{-1} (Figure 6a). Second, given different closure temperatures and ages for the three thermochronometers, sample cooling rates can be calculated over different time intervals. The Syange South and North data show that the samples cooled from 90°C (AHe closure temperature (ct)) to the surface at rates ranging from ~100 to 270°C Myr^{-1}, from 140° to 90°C (AFT ct to AHe ct) at rates of 30 to 170°C Myr^{-1} and from 330 to 250° to 140°C (ZFT ct to AFT ct) at a rate of >500°C Myr^{-1}. We cannot readily reconcile these contradictions and attribute them in part to the large uncertainties assigned to the fission track ages.

4.2.1.5. Syange North

[27] A few kilometers north of the Syange South transect, an additional three samples were collected from the ridgeline rising to ~2.8 km elevation (Figure 2b). Despite large errors associated with each apatite fission track age (Figure 6b), the calculated exhumation rate ($1.5^{+inf}_{-1.0}$ km Myr^{-1}) is the same as that calculated for Syange South (Figure 6a). Two zircon fission track ages and one apatite He age were also obtained

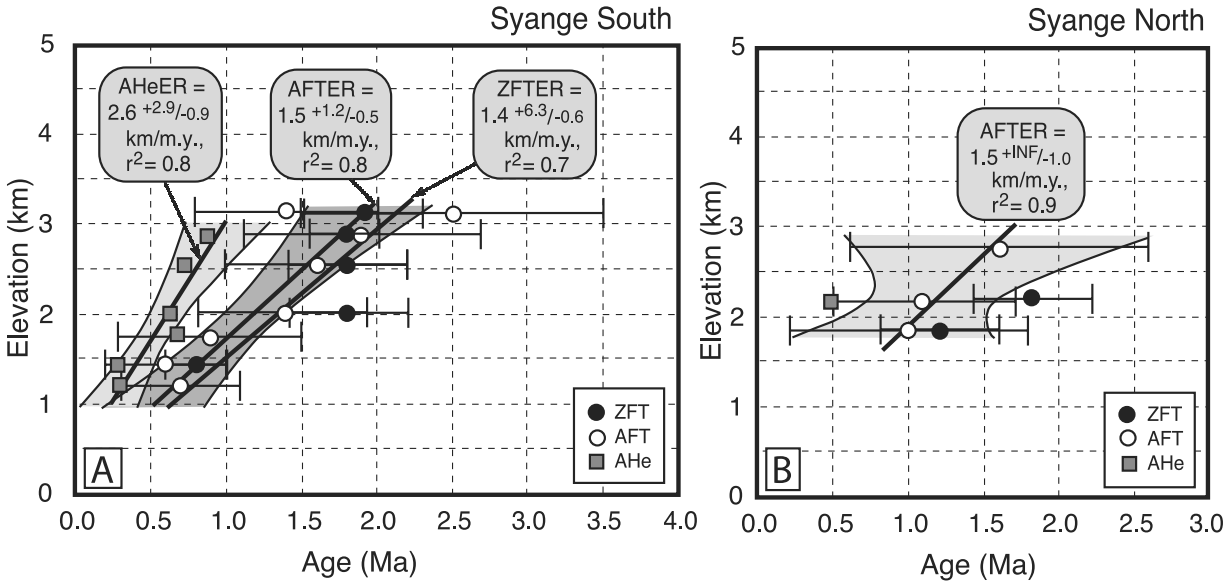

Figure 6. Apatite fission track ages plotted against sample elevations for samples collected on two vertical relief transects: (a) Syange South and (b) Syange North. These two transects also have zircon fission track and apatite (U-Th)/He ages plotted for several of the same samples. Lines define mean exhumation rates calculated using an error-weighted least squares linear regression; 95% confidence intervals are shown. See Figure 2b for transect locations and the text for further discussion.

from these samples, confirming the patterns seen at Syange South.

4.2.2. North-South, Transport-Parallel, Strike-Perpendicular Transects

4.2.2.1. Bagarchhap

[28] Bagarchhap and Chame are transport-parallel transects that dip toward the north, approximately parallel to particle paths through the orogen. In theory, a section with this orientation should provide the most readily interpretable rate information, because all samples should have crossed the closure isotherm in nearly the same place (Figure 4). Four samples were collected on a transect that ascends southward beginning near Bagarchhap (Figure 2b). The transect spans 1800 m over a 4.3 km distance and dips $\sim$20° toward the north. The lowest sample yielded no tracks (an age of 0.0 Ma if calculated as a central age) and may possibly have been reset by hydrothermal waters, given that hot springs are scattered along this stretch of the Marsyandi. The true "age" of this sample is difficult to evaluate: *Galbraith* [2005] suggests that the 0-track analysis should be treated as a range of ages within the 95% confidence interval. In this case the possible age lies between 0 and $\sim$0.4 Ma. This analysis, without an actual age, is therefore excluded from the exhumation rate calculation (Figure 7a). For the Bagarchhap area, we obtain a mean exhumation rate of $4.2^{+\mathrm{inf}}_{-3.2}$ km Myr^{-1}.

4.2.2.2. Chame

[29] The transect ascending southward from Chame (Figure 2b) in the northwestern part of the field area yielded the most disparate pattern of ages for any transect within this study. Seven samples were collected along a 5.5-km transect spanning over $\sim$1.8 km of elevation and dipping $\sim$18° to the north. Three of the four upper samples had very large errors, whereas the third highest sample yielded the youngest age of the seven samples with a relatively small error (0.3 ± 0.2 Ma, Figure 7b). This young, high-elevation age perturbs the error-weighted regression such that the calculated exhumation rate is negative: $-11^{+13}_{-3.2}$ km Myr^{-1} (Figure 7b). Although the rate itself is unrealistic, the data suggest that the exhumation rate is sufficiently rapid here and errors on ages are sufficiently large that no discernible age-elevation trend is found. This transect is complicated by the location of the Phu Detachment (Figure 2), which has been mapped nearby [*Searle and Godin*, 2003], although the exact location with respect to our samples is unknown.

4.2.2.3. Khudi Ridges and Nagi Lek

[30] In the southern part of the study area, three strike-perpendicular ridges occur approximately parallel to the main Marsyandi trunk stream. Two of the ridges define the east and west margins of the Khudi catchment to the west of the Marsyandi, whereas the Nagi Lek ridge borders the Marsyandi along its east bank (Figure 2a). Samples were collected along all three ridges (Figure 8). Samples from the Khudi East ridge were previously discussed as defining the top of the Syange east-west transect (Figure 6a). In long profile, all three ridges appear topographically similar (Figure 9a), and each displays steep, linear slopes that rise $\sim$2 km above adjacent valley bottoms (Figure 9c). Nine samples collected along the Khudi West ridge span $\sim$2.4 km of elevation and $\sim$15 km of horizontal distance (Figure 2a), so that the ridge crest slopes south at $\sim$9°. Despite the average 2 km of relief from the valley bottoms where the

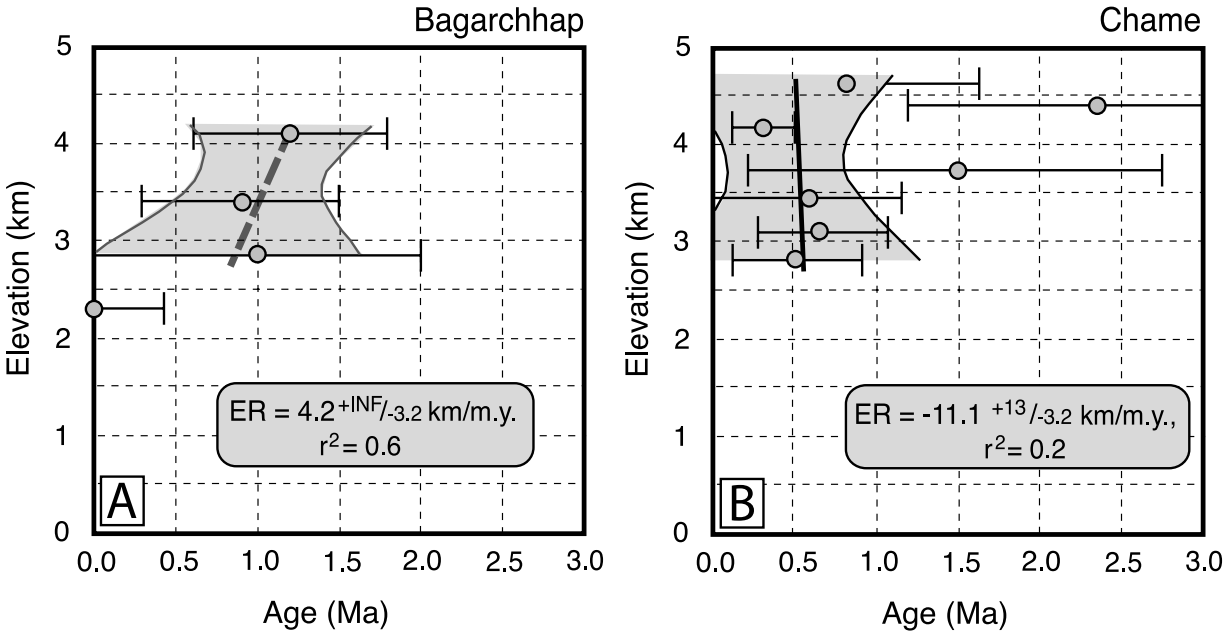

Figure 7. Apatite fission track ages plotted against sample elevations for two, north sloping strike-parallel transects: (a) Bagarchhap and (b) Chame. Lines defining mean exhumation rates calculated using an error-weighted least squares linear regression and 95% confidence intervals are shown. See Figure 2b for transect locations and the text for further discussion.

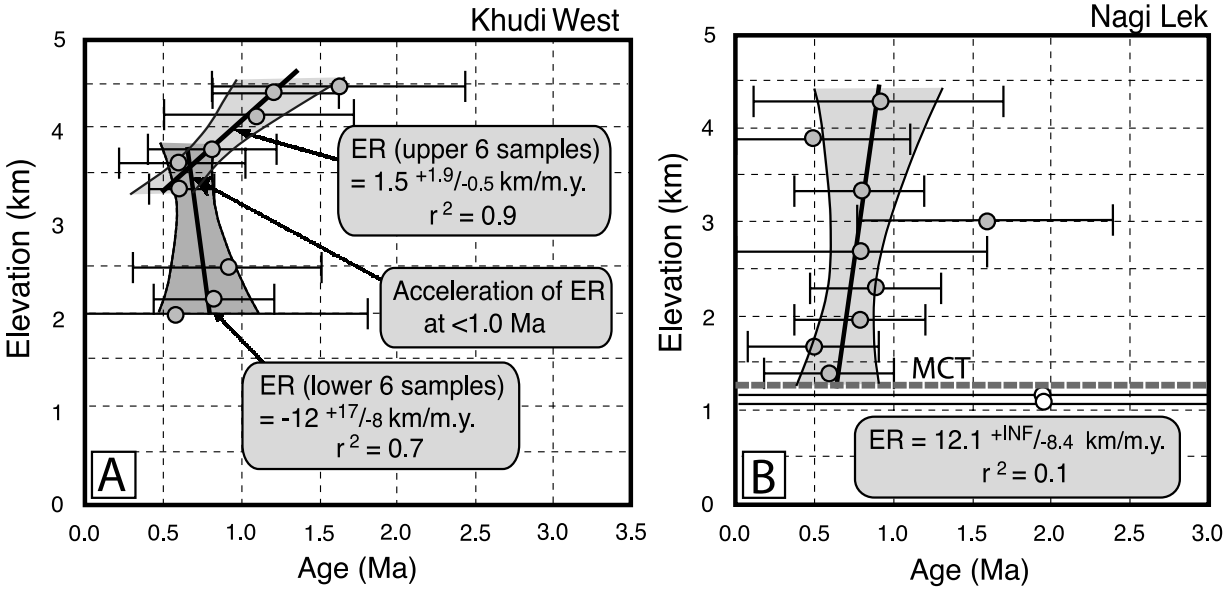

Figure 8. Apatite fission track ages plotted against sample elevations for south sloping strike-perpendicular ridges. Lines define mean exhumation rates calculated using an error-weighted least squares linear regression; 95% confidence intervals are shown. (a) Khudi West ages can be interpreted as encompassing an upper group of more slowly eroding ages above a lower group representing very rapid exhumation since <1 Ma. The ages between 3800 to 3300 m were used in both regressions. (b) Basal Nagi Lek dates in the footwall of the MCT have large uncertainties, but appear offset from the ages in the hanging wall, suggesting Quaternary slip on the MCT. A very rapid exhumation rate is interpreted for the hanging wall. Even 2–3 km above the valley bottom, cooling ages are <1 Ma.

samples were collected, the nine apatite ages average 0.9 ± 0.4 Ma (Figures 9b and 9c). If these samples are interpreted as a vertical relief transect, an intriguing pattern emerges because they can be divided into two groups (Figure 8a). Between about 4500 and 3500 m elevation, the upper six samples yield an exhumation rate of ~1.5 km Myr^{-1} for the time period from ~1.6 to 0.6 Ma (r^2 = 0.89). In contrast, the samples below ~3500 m are all approximately the same age and predict a very rapid exhumation rate (indistinguishable from infinite, Figure 8a). The bend at the base of the more slowly cooled samples mimics the pattern that is typically found at the base of an uplifted partial annealing zone [*Fitzgerald et al.*, 1995; *Stockli et al.*, 2000] and is commonly interpreted to indicate the time of an acceleration in denudation rates. In this context, the trend in the Khudi West data could indicate that such an acceleration began at <1 Myr. This inference is consistent with the interpretation of the Syange South transect for accelerated exhumation at roughly the same time.

[31] The Nagi Lek ridgeline has a south-southwesterly trend (Nagi Lek is the name of the highest peak in this ridgeline), whereas the Jagat sampling transect ascends the west flank of the Nagi Lek ridge, includes some of the Nagi Lek ridgeline samples, and is more nearly perpendicular to the Marsyandi drainage. Eleven samples were collected along the Nagi Lek ridgeline descending to the Marsyandi River and spanning ~3 km of elevation across a horizontal distance of ~14 km. The lower six of these samples were previously published by *Huntington et al.* [2006]. On average, the ridge slopes southward at ~13°. The two lowermost Nagi Lek samples, each with ages of 1.9 ± 2.2 Ma near river level, appear to be offset from the higher samples by a splay of the Main Central Thrust (the Nalu thrust of *Hodges et al.* [2004]). This offset suggests that slip has occurred on this thrust in the past 1 Myr. When interpreted as a vertical relief section, the nine samples in the hanging wall predict a high exhumation rate of $12^{+inf}_{-8.4}$ km Myr^{-1} (Figure 8b). Given that the Jagat transect ascends the flank of the Nagi Lek ridge, we would expect them to have similar exhumation rates. Although the $5.7^{+inf}_{-2.9}$ km Myr^{-1} for Jagat and the $12^{+inf}_{-8.4}$ km Myr^{-1} for Nagi Lek overlap, the differences between them indicate the level of uncertainty in interpreting these data.

[32] The most intriguing aspect of these three strike-perpendicular ridges is that despite their morphological

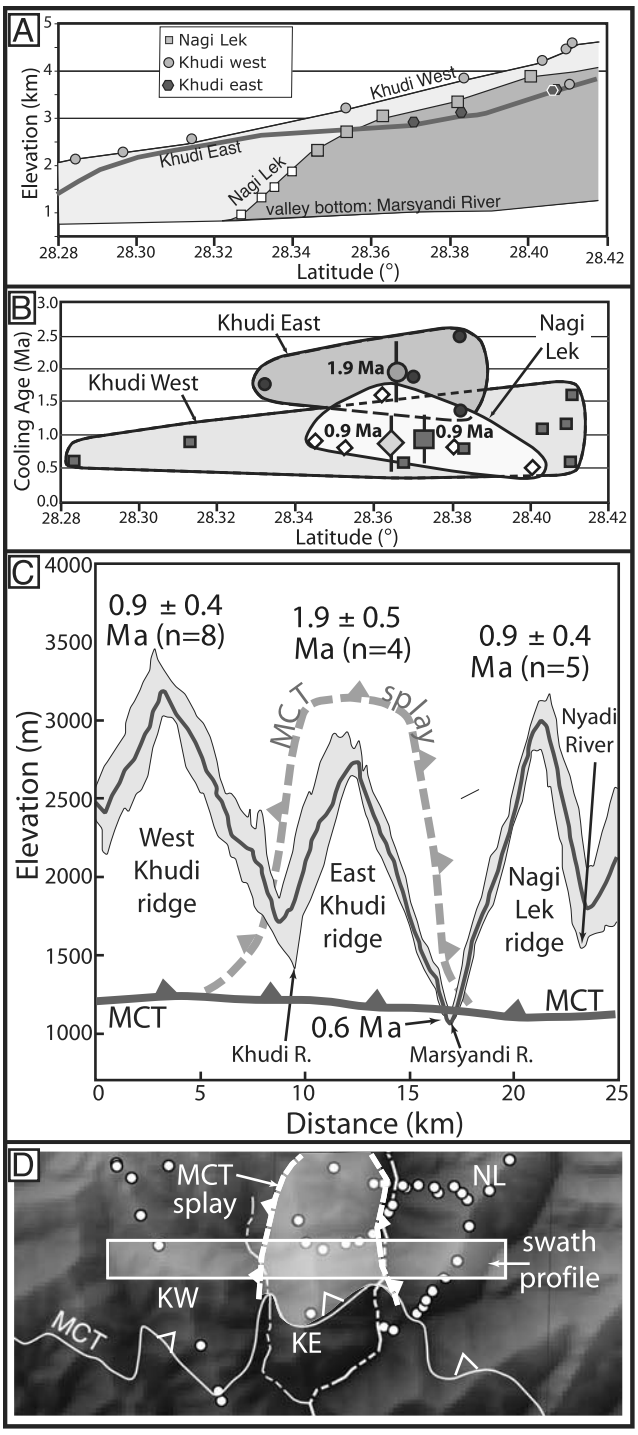

Figure 9. Comparison of three strike-perpendicular ridges. (a) Topographic profiles of the Khudi West, Khudi East, and Nagi Lek ridges, with sample locations along their crests indicated. (b) Groupings of cooling ages in each ridge crest. The large symbols indicate the mean age for each sample set. The Nagi Lek samples indicated by open boxes on Figure 9a are not included in the ridge crest averages because they descend steeply to the Marsyandi River. Despite similar topography, the Khudi West and Nagi Lek ridges have much younger ages than the Khudi East ridge. (c) Maximum, minimum, and mean topography from an east-west swath across the southern part of all three ridges. Each ridge is flanked by linear, steep slopes with ~2 km of relief. Despite being lower, Khudi East ridge has older ages, indicating slower overall exhumation rates. Note that for Nagi Lek, the age difference from the valley bottom to the crest is only ~0.3 My across 2 km of relief. Speculative position of a splay branching from the MCT is shown. (d) Sample and topographic swath locations for the three ridges. The speculative trace of a splay of the MCT that has isolated the Khudi East region is depicted.

similarity and comparable orientations, they display some striking contrasts in the cooling ages along their crests (Figures 9b and 9c). Whereas the Khudi West and Nagi Lek ridges have mean ages of 0.9 ± 0.4 Ma for 13 samples along their crests, the Khudi East ridge has a mean age of 1.9 ± 0.5 Ma. Thus, on average, the topographically lower ridge has ages twice as old as the adjacent higher ridges: a trend exactly opposite to that expected in a region with a spatially uniform exhumation history. In fact, the Khudi East ridge and the Syange transects stand out as anomalies because their interpreted exhumation rates are considerably slower than those of the other transects. We therefore suggest that the Khudi East area represents a region that has been somewhat structurally isolated from the neighboring terrain, by a splay of the Main Central Thrust that lies above the ridge (Figure 9d). Quaternary slip along this splay could have generated young cooling ages in the hanging wall, whereas the footwall (Khudi East) experienced considerably slower exhumation prior to ~0.6–0.8 Ma. No mapped structure is known to correspond to the speculative fault geometry, but knickpoints (Figure 2a) along the Khudi River [*Hodges et al.*, 2004] and the contrast in cooling ages between the Syange and Jagat transects (Figure 2b) may indicate the hypothesized fault's location (Figure 9d).

5. Discussion

[33] The apatite fission track data described here represent the most focused and altitudinally diverse archive of low-temperature bedrock cooling ages in the Himalaya. The sheer number of transects and the overall density of sampling within this rugged terrain render this a unique data set. Although some transects (e.g., Syange and Khudi West) display systematic trends toward older ages with increasing altitude, for many transects, the ages of high-elevation samples differ little from those at the valley bottoms: an indication of the overall rapidity of exhumation. Indeed, one of the striking overall observations of the data presented here is just how young they are. Several of the zircon fission track, most of the apatite fission track, and all of the apatite (U-Th)/He ages are less than 1 Ma. These ages are, in general, substantially younger than those seen elsewhere in a similar structural position (Greater Himalaya and Tethyan strata) within the Himalaya [e.g., *Jain et al.*, 2000; *Kumar et al.*, 1995; *Thiede et al.*, 2004, 2005; *Vannay et al.*, 2004], with the exception of the Goriganga valley in the central Himalaya [*Bojar et al.*, 2005] and the Himalayan syntaxes, such as at Namche-Barwa, where similarly young ages have been obtained [*Burg et al.*, 1997; *Seward et al.*, 2004]. This orogen-wide variation in ages suggests that despite the remarkable structural homogeneity along strike within the Himalaya, substantial lateral variations exist in rates of processes, either exhumational or tectonic, or both.

[34] On the basis of the above described spatial patterns (Figure 2b) and age-versus-elevation relationships for the fission track and (U-Th)/He analyses, our assessment of the overall pattern of exhumation over the last 1–2 Myr indicates that within the Marsyandi catchment, much of the Greater Himalaya and parts of southern Tibet were being exhumed at rates exceeding 1.5 mm yr^{-1}. Our analysis, however, takes no account of the topographic perturbation of isotherms [e.g., *Manktelow and Grasemann*, 1997], and instead assumes a parallel closure isotherm in the age-elevation analyses. Clearly, the combination of striking relief with high exhumation rates will cause a significant upward perturbation of isotherms beneath ridge crests. Hence, because of the shortened distance to the surface from the perturbed reference isotherm, true vertical exhumation rates may be lower than those estimated here. *Whipp et al.* [2007] apply thermokinematic modeling to these data to better evaluate these effects.

[35] With these caveats in mind, we interpret the overall pattern of exhumation rates for all of the transects in the Annapurna region as follows:

[36] 1. From 2 to ~0.8 Ma, exhumation rates appear to have been ~1.5 km Myr^{-1}. These rates were primarily quantifiable for the Syange South and North vertical relief transects in the southern part of the field area, where ages were older than those from the rest of the study area, and the r^2 values, measuring the likelihood that the age/elevation data points represented a linear trend, were high (>0.7). Rates derived from the zircon and apatite fission track data from the Syange samples are nearly identical (~1.5 and 1.4 km Myr^{-1}) for the time period from ~2 to 0.8 Myr. The upper six samples in the Khudi West transects define a similar rate prior to an acceleration after ~0.8 Ma. All of the other elevation transects had significantly younger ages (and much lower r^2 values), even at much higher elevations. The rate we obtained for this time period is rapid, but not exceptional: similar rates have been obtained in the Sutlej and Kishtwar regions of northwestern India [*Kumar et al.*, 1995; *Jain et al.*, 2000; *Thiede et al.*, 2004, 2005].

[37] 2. In comparison to the previous million years, our data suggest a significant acceleration in exhumation rates after ~0.8 Ma. From ~0.8 to 0.5 Myr, many age-elevation trends suggest exhumation rates of ~2 to 5 km Myr^{-1}. A relatively robust exhumation rate (with r^2 values >0.7) for 0.8 to 0.5 Myr, of 2.6 km Myr^{-1}, was obtained from Syange South with apatite (U-Th)/He analyses. Rates exceeding ~4 km Myr^{-1} are also calculated for Chame, Nagi Lek, Jagat, Dharapani, and lower Khudi West for this same interval, but with greater scatter in the data (with r^2 values <0.4).

[38] 3. From 0.5 Ma to the present, exhumation rates were also ~2 to 5 km Myr^{-1}. The mean apatite fission track age from river level samples is 0.6 ± 0.3 Ma. We estimate the exhumation rate over the last ~0.5 Myr with this mean age and an assumed closure temperature and geothermal gradient. For this calculation, we assume a geothermal gradient of 50–100°C km^{-1}, an apatite fission track closure temperature of 140°C, and mean annual temperature of 10°C. The assumption of a high geothermal gradient of 50 to 100°C km^{-1} is probably appropriate, based on rapid vertical advection of heat in the crust that would occur during rapid denudation and on the presence of hot springs along the valley bottom [*Craw et al.*, 1994]. A high apatite fission track closure temperature of ~140°C is based on the high cooling rate (>200°C Myr^{-1}) indicated by the very young apatite fission track ages. A mean annual temperature

of ~10°C is used, based on the values measured at the village of Tal in the middle of the field area. With these numbers, we calculate exhumation rates of 2.2 to 4.6 km Myr^{-1}. Using the same variables and a closure temperature of 90°C, the (U-Th)/He apatite age (0.3 Ma) from the lowest sample indicates an exhumation rate of 2.7 km Myr^{-1} for a geothermal gradient of 100°C and 5 km Myr^{-1} for one of 50°C. Thus the calculated rates for both apatite (U-Th)/He and fission track methods are equivalent and rapid. These rates are similar to the rates obtained from vertical transects for 0.8 to 0.5 Ma, and they suggest that no dramatic change in regional exhumation rates has occurred in the last 0.7 to 0.8 Myr.

[39] The oldest apatite fission tract ages are recorded in the region of Khudi East ridge and the Syange transects along the west side of the lower Marsyandi River. Whereas the river level sample ages (~0.6 Ma) are consistent with exhumation rates >2.2 km Myr^{-1} over this time interval, the overlying rocks preserve ages exceeding 1–2 Ma and define a slower exhumation rate of ~1.5 km Myr^{-1}. The only other place where such a rate can be documented is in the adjacent Khudi West ridge, but there, rocks with the relevant ages are found at elevations >2 km higher than at Khudi East (Figure 9). We suggest that differential uplift due to slip on a splay above the MCT offset these two transects.

[40] The data presented here suggest that exhumation rates in the Marsyandi region increased sometime after 1 Ma, either as the result of regionally increased tectonic rates, locally active faulting, or a change in climatic conditions causing increased exhumation rates. Around 900 ka, glacial-interglacial cycles switched from a 40-kyr periodicity to an ~100-kyr periodicity and ice sheets with larger volumes developed in the Northern Hemisphere [*Shackleton and Opdyke*, 1976]. Exhumation rates in alpine regions, including the Himalaya, may have accelerated at this time. In the Bengal Fan, sediment accumulation rates increased after ~1 Ma [*Shipboard Scientific Party*, 1989], and a coeval switch occurred in the dominant clay from smectite to illite [*Derry and France-Lanord*, 1996]. Both trends can be interpreted as a response to an increase in the rate of physical exhumation in the Himalaya [*Derry and France-Lanord*, 1996].

[41] Although an increase in physical exhumation rates is consistent with our observed acceleration in rates of cooling, climate change is only one possible cause. Our data showing rocks in the hanging wall of the MCT with cooling ages of ~0.5 Ma thrust over footwall rocks with ages of ~2 Ma suggest that slip also occurred on the MCT during the past 1 Myr (Figure 8b). Slip rates of several mm yr^{-1} could also account for the observed offset in ages across the MCT. If such faulting did occur in this time interval, it would be expected to drive accelerated rates of exhumation and cooling in its hanging wall.

[42] Finally, we see no obvious link between present-day climate (precipitation) and exhumation patterns. In this south-to-north transect along the Marsyandi drainage, the amount of precipitation varies by approximately tenfold. On the basis of apatite fission track ages from the bottom of the Marsyandi gorge in the Greater Himalaya, *Burbank et al.* [2003] argued that there was no correlation between the pattern of precipitation and exhumation, as interpreted from cooling rates obtained from apatite FT analyses. Across the Greater Himalaya itself, monsoonal rainfall decreases approximately fourfold, whereas the valley bottom ages trend younger to the north and the vertical relief transects argue for comparable rates in the northern part of the Greater Himalaya. The fission track data in this study also extend the original valley bottom data set another 25 km to the north across the semiarid zone of Tethyan strata to the north of the South Tibetan Detachment. These data reveal ages that are on average older and probably indicate slower exhumation. Whether this is a climatic effect, is a response to slip on the South Tibetan Detachment, or simply indicates a smaller vertical component of hanging wall uplift above a less steeply dipping segment of the Main Himalayan Thrust remains undetermined.

6. Conclusions

[43] The large database of apatite and zircon fission track and apatite (U-Th)/He analyses presented here allows us to characterize the cooling and exhumation history of the Annapurna region in central Nepal. The AFT ages obtained in this study are, in general, younger than ages obtained from regions in a structurally similar position throughout the Himalaya, except at the syntaxes. We infer that these ages indicate Quaternary exhumation rates across the Greater Himalaya and southern Tibet in the Marsyandi catchment that were, on average, higher than anywhere else along the Himalaya other than at the termini where very large rivers (Indus and Tsangpo) cut across the range. Data from a small subset of the overall samples suggest that exhumation rates were ~1.5 km Myr^{-1} from 2 to 0.8 Myr. Rates appear to have accelerated during the last 0.8 Myr, and probably ranged from 2.5 to 5 km Myr^{-1}, either as the result of a long-term change in climate, and/or an increase in fault activity on the Main Central Thrust, which appears to have been active during the past ~1 Myr in the Annapurna region. An apparent offset of apatite fission track ages occurs across the MCT in the southern part of the field area. In addition, abrupt spatial contrasts in exhumation rates as deduced from vertical relief sections suggests that a northerly splay, which probably branches from the Main Central Thrust, may have insulated a footwall block from rapid exhumation during the Quaternary. Finally, despite a fourfold northward decrease in monsoon rainfall within the Greater Himalaya, our relief transects and valley bottom dates indicate that long-term exhumation rates do not discernibly decrease. Within the Tethyan strata farther north, rates appear somewhat slower, perhaps due to tectonic causes (slip on the South Tibetan Detachment or a less steep Main Himalayan Thrust beneath southern Tibet) or in response to the drier climate. The paper that follows [*Whipp et al.*, 2007] uses thermokinematic modeling to further evaluate these data. The large uncertainties as a fraction of the age for these young apatite fission track samples make an unequivocal assessment of spatial variations in exhumation rates difficult to achieve. Improvements in

understanding of changes in rates will likely emerge from use of low-temperature thermochronometers with higher precision and collection of more vertical relief transects within the Tethyan realm. In addition, determination of (1) rates of Quaternary slip on the South Tibetan Detachment, (2) the geometry of the underlying sole thrust, and (3) the role of glacial exhumation will help to evaluate interactions among climate, exhumation, and tectonics within the Tethyan realm.

[44] **Acknowledgments.** This research was funded by NSF grant EAR-9909488. Field assistance was provided by Tank Ohja and Himalayan Experience of Kathmandu, Nepal. Ian Brewer and Beth Pratt-Sitaula collected additional samples. We thank Ken Farley and Lindsey Hedges for assistance with (U-Th)/He thermochronometry; Jeremy Zechar, Kip Hodges, and Kate Ruhl-Huntington for discussions about statistics; and Colin Amos for help with DEM analyses. Reviews by Trevor Dumitru and Kerry Gallagher substantially improved the manuscript and were greatly appreciated.

References

Arita, K., and Y. Ganzawa (1997), Thrust tectonics and uplift process of the Nepal Himalaya revealed from fission-track ages, *J. Geogr. Jpn.*, *106*, 156–167.

Barros, A. P., and T. J. Lang (2003), Monitoring the monsoon in the Himalayas: Observations in central Nepal, *Mon. Weather Rev.*, *131*, 1408–1427.

Beaumont, C., R. A. Jamieson, M. H. Nguyen, and B. Lee (2001), Himalayan tectonics explained by extrusion of a low-viscosity crustal channel coupled to focused surface denudation, *Nature*, *414*, 738–742.

Besse, J., and V. Courtillot (1988), Paleogeographic maps of the Indian Ocean bordering continents since the upper Jurassic, *J. Geophys. Res.*, *93*, 11,791–11,808.

Bojar, A.-V., H. Fritz, S. Nicolescu, M. Bregar, and R. P. Gupta (2005), Timing and mechanisms of central Himalayan exhumation: Discriminating between tectonic and erosion processes, *Terra Nova*, *17*, 427–433.

Bookhagen, B., and D. W. Burbank (2006), Topography, relief, and TRMM-derived rainfall variations along the Himalaya, *Geophys. Res. Lett.*, *33*, L08405, doi:10.1029/2006GL026037.

Bookhagen, B., R. Thiede, and M. R. Strecker (2004), Late Quaternary intensified monsoon phases control landscape evolution in the northwest Himalaya, *Geology*, *33*, 149–152.

Brewer, I. D., and D. W. Burbank (2006), Thermal and kinematic modeling of bedrock and detrital cooling ages in the central Himalaya, *J. Geophys. Res.*, *111*, B09409, doi:10.1029/2004JB003304.

Brewer, I. D., D. W. Burbank, and K. V. Hodges (2003), Modelling detrital cooling-age populations: Insights from two Himalayan catchments, *Basin Res.*, *15*, 305–320.

Burbank, D. W., and R. S. Anderson (2001), *Tectonic Geomorphology*, 1st ed., 273 pp., Blackwell Sci., Malden, Mass.

Burbank, D. W., A. E. Blythe, J. Putkonen, B. Pratt-Sitaula, E. Gabet, M. Oskin, A. Barros, and T. Ohja (2003), Decoupling of erosion and precipitation in the Himalayas, *Nature*, *426*, 652–655.

Burg, J. P., P. Davy, P. Nievergelt, F. Oberli, D. Seward, Z. Diao, and M. Meier (1997), Exhumation during crustal folding in the Namche-Barwa syntaxis, *Terra Nova*, *9*, 53–56.

Catlos, E. J., T. M. Harrison, M. J. Kohn, M. Grove, F. J. Ryerson, C. E. Manning, and B. N. Upreti (2001), Geochronologic and thermobarometric constraints on the evolution of the Main Central Thrust, central Nepal Himalaya, *J. Geophys. Res.*, *106*(B8), 16,177–16,204.

Colchen, M., P. LeFort, and A. Pêcher (1986), *Annapurna-Manaslu-Ganesh Himal*, 136 pp., Centre Natl. de la Rec. Sci., Paris.

Coleman, M. E. (1996), The tectonic evolution of the central Himalaya, Marsyandi Valley, Nepal, Ph.D. thesis, 221 pp., Mass. Inst. of Technol., Cambridge.

Coleman, M. E., and K. V. Hodges (1998), Contrasting Oligocene and Miocene thermal histories from the hanging wall and footwall of the south Tibetan detachment in the central Himalaya from $^{40}Ar/^{39}Ar$ thermochronology, Marsyandi Valley, central Nepal, *Tectonics*, *17*, 726–740.

Craw, D., P. O. Koons, D. Winslow, C. P. Chamberlain, and P. Zeitler (1994), Boiling fluids in a region of rapid uplift, Nanga Parbat Massif, Pakistan, *Earth Planet. Sci. Lett.*, *128*, 169–182.

Dadson, S. J., et al. (2003), Links between erosion, runoff variability and seismicity in the Taiwan orogen, *Nature*, *426*, 648–651.

Derry, L. A., and C. France-Lanord (1996), Neogene Himalayan weathering history and river $^{87}Sr/^{86}Sr$: Impact on the marine Sr record, *Earth Planet. Sci. Lett.*, *142*, 59–76.

Dodson, M. H. (1973), Closure temperature in cooling geochronological and petrological systems, *Contrib. Mineral. Petrol.*, *40*, 259–274.

Dumitru, T. A. (1993), A new computer automated microscope stage system for fission-track analysis, *Nucl. Tracks Radiat. Meas.*, *21*, 575–580.

Dumitru, T. A. (2000), Fission-track geochronology, in *Quaternary Geochronology: Methods and Applications*, *Ref. Shelf*, vol. 4, edited by J. S. Noller, J. M. Sowers, and W. R. Lettis, pp. 131–156, AGU, Washington, D. C.

Dunkl, I. (2002), TRACKKEY: A Windows program for calculation and graphical presentation of fission track data, *Comput. Geosci.*, *28*, 3–12.

Farley, K. A. (2000), Helium diffusion from apatite: General behavior as illustrated by Durango fluorapatite, *J. Geophys. Res.*, *95*, 2903–2914.

Fitzgerald, P. G., and A. J. W. Gleadow (1988), Fission track geochronology, tectonics and structure of the Transantarctic Mountains in northern Victoria Land, Antarctica, *Isotope Geoscience*, *73*, 19–169.

Fitzgerald, P. G., R. B. Sorkhabi, T. F. Redfield, and E. Stump (1995), Uplift and denudation of the central Alaska Range: A case study in the use of apatite fission track thermochronology to determine absolute uplift parameters, *J. Geophys. Res.*, *100*, 20,175–20,191.

Galbraith, R. F. (1981), On statistical methods of fission track counts, *Math. Geol.*, *13*, 471–478.

Galbraith, R. F. (1990), The radial plot: Graphical assessment of the spread in ages, *Nucl. Tracks Radiat. Meas.*, *17*, 207–214.

Galbraith, R. F. (2005), *Statistics for Fission Track Analysis*, 50–52 pp., CRC Press, Boca Raton, Fla.

Gleadow, A. J. W., and P. G. Fitzgerald (1987), Uplift history and structure of the Transantarctic Mountains: New evidence from fission track dating of basement apatites in the Dry Valleys area, southern Victoria Land, *Earth Planet. Sci. Lett.*, *82*, 1–14.

Green, P. F. (1981), A new look at statistics in fission track dating, *Nucl. Tracks*, *5*, 77–86.

Green, P. F., I. R. Duddy, A. J. W. Gleadow, P. R. Tingate, and G. M. Laslett (1986), Thermal annealing of fission tracks in apatite: 1, A qualitative description., *Chem. Geol.*, *59*, 237–253.

Grujic, D., I. Coutand, B. Bookhagen, S. Bonnet, A. Blythe, and C. Duncan (2006), Climatic forcing of erosion, landscape, and tectonics in the Bhutan Himalayas, *Geology*, *34*, 801–804, doi:10.1130/G22648.1.

Harrison, T. M., F. J. Ryerson, P. LeFort, A. Yin, O. M. Lovera, and E. J. Catlos (1997), A late Miocene-Pliocene origin for the central Himalayan inverted metamorphism, *Earth Planet. Sci. Lett.*, *146*, E1–E7.

Hodges, K. V. (2000), Tectonics of the Himalaya and southern Tibet from two perspectives, *Geol. Soc. Am. Bull.*, *112*, 324–350.

Hodges, K. V., J. M. Hurtado, and K. X. Whipple (2001), Southward extrusion of Tibetan crust and its effect on Himalayan tectonics, *Tectonics*, *20*, 799–809.

Hodges, K. V., C. Wobus, K. Huntington, T. Schildgen, and K. Whipple (2004), Quaternary deformation, river steepening, and heavy precipitation at the front of the Higher Himalayan ranges, *Earth Planet. Sci. Lett.*, *220*, 379–389.

Huntington, K. W., and K. V. Hodges (2006), A comparative study of detrital mineral and bedrock age-elevation methods for estimating erosion rates, *J. Geophys. Res.*, *111*, F03011, doi:10.1029/2005JF000454.

Huntington, K., A. Blythe, and K. Hodges (2006), Climate change and late Pliocene acceleration of erosion in the Himalaya, *Earth Planet. Sci. Lett.*, *252*, 107–118.

Hurford, A. J., and P. F. Green (1983), The Zeta age calibration of fission-track dating, *Isotope Geosci.*, *1*, 285–317.

Hurtado, J. M., K. V. Hodges, and K. X. Whipple (2001), Neotectonics of the Thakkhola Graben and implications for Recent activity on the South Tibetan Fault System in the central Nepalese Himalaya, *Geol. Soc. Am. Bull.*, *113*, 222–240.

Jain, A. K., D. Kumar, S. Singh, A. Kumar, and N. Lal (2000), Timing, quantification and tectonic modelling of Pliocene-Quaternary movements in the NW Himalaya: Evidence from fission track dating, *Earth Planet. Sci. Lett.*, *179*, 437–451.

Ketcham, R., R. A. Donelick, and W. D. Carlson (1999), Variability of apatite fission-track annealing kinetics: III. Extrapolation to geologic time scales, *Am. Mineral.*, *84*, 1235–1255.

Kumar, A., N. Lal, A. K. Jain, and R. S. Sorkhabi (1995), Late Cenozoic Quaternary thermotectonic history of Higher Himalayan crystalline in Kishtwar-Padar-Zanskar region, NW Himalaya: Evidence from fission track ages, *J. Geol. Soc. India*, *45*, 375–391.

Lavé, J., and J. P. Avouac (2000), Active folding of fluvial terraces across the Siwalik Hills, Himalayas of central Nepal, *J. Geophys. Res.*, *105*, 5735–5770.

Ludwig, K. (2003), Isoplot 3.0.A geochronological toolkit for Microsoft Excel, *Spec. Publ. 4*, 73 pp., Berkeley Geochronol. Center, Berkeley, Calif.

Manktelow, N. S., and B. Grasemann (1997), Time-dependent effects of heat advection and topography on cooling histories during erosion, *Tectonophysics*, *270*, 167–195.

Martin, A. J., P. G. DeCelles, G. E. Gehrels, P. J. Patchett, and C. Isachsen (2005), Isotopic and structural constraints on the location of the Main Central thrust in the Annapurna Range, central Nepal Himalaya, *Geol. Soc. Am. Bull.*, *117*, 926–944.

Meigs, A. J., D. W. Burbank, and R. A. Beck (1995), Middle–late Miocene (>10 Ma) formation of the Main Boundary thrust in the western Himalaya, *Geology*, *23*, 423–426.

Molnar, P., and P. England (1990), Late Cenozoic uplift of mountain ranges and global climate change: Chicken and egg?, *Nature*, *346*, 29–34.

Naeser, C. W. (1979), Fission track dating and geologic annealing of fission tracks, in *Lectures in Isotope Geology*, edited by E. Jäger and J. C. Hunziker, pp.154–169, Springer, New York.

Pandey, M. R., R. P. Tandukar, J. P. Avouac, J. Lave, and J. P. Massot (1995), Interseismic strain accumulation on the Himalayan crustal ramp (Nepal), *Geophys. Res. Lett.*, *22*, 751–754.

Rahn, M. K., M. T. Brandon, G. E. Batt, and J. I. Garver (2004), A zero-damage model for fission-track annealing in zircon, *Am. Mineral.*, *89*, 473–484.

Reiners, P., T. A. Ehlers, S. G. Mitchell, and D. R. Montgomery (2003), Coupled spatial variations in precipitation and long-term erosion rates across the Washington Cascades, *Nature*, *426*, 645–647.

Rowley, D. B. (1996), An age of initiation of collision between India and Asia: A review of the stratigraphic record, *Earth Planet. Sci. Lett.*, *145*, 1–13.

Searle, M. P., and L. Godin (2003), The South Tibetan Detachment and the Manaslu Leucogranite: A structural reinterpretation and restoration of the Annapurna-Manaslu Himalaya, Nepal, *J. Geol.*, *111*, 505–523.

Seeber, L., J. G. Armbruster, and R. C. Quittmeyer (1981), Seismicity and continental subduction in the Himalayan arc, in *Zagros, Hindu Kush, Himalaya—Geodynamic Evolution*, *Geodyn. Ser.*, vol. 3, edited by H. K. Gupta and F. M. Delaney, pp. 215–242, AGU, Washington, D. C.

Seward, D., et al. (2004), The eastern syntaxis of the Himalaya—Exhumation studies and erosion, paper presented at 10th International Conference on Fission-Track Dating and Thermochronology, Vrije Univ., Amsterdam.

Shackleton, N. J., and N. D. Opdyke (1976), Oxygen-isotopes and paleomagnetic stratigraphy of Pacific core V28–239 late Pliocene to latest Pleistocene, *Mem. Geol. Soc. Am.*, *145*, 449–464.

Shipboard Scientific Party (1989), Initial reports sites 717–718–719 Distal Bengal Fan, *Proc. Ocean Drill. Program Initial Rep.*, *116*.

Stockli, D., K. A. Farley, and T. A. Dumitru (2000), Calibration of the apatite (U-Th)/He thermochronometer on an exhumed fault block, White Mountains, California, *Geology*, *28*, 983–986.

Tagami, T., and T. A. Dumitru (1996), Provenance and thermal history of the Franciscan accretionary complex: Constraints from fission track thermochronology, *J. Geophys. Res.*, *101*, 11,353–11,364.

Tagami, T., A. Carter, and A. J. Hurford (1996), Natural long-term annealing of the zircon fission-track system in Vienna Basin deep borehole samples: Constraints upon the partial annealing zone and closure temperature, *Chem. Geol.*, *130*, 147–157.

Tagami, T., R. F. Galbraith, R. Yamada, and G. M. Laslett (1998), Revised annealing kinetics of fission-tracks in zircon and geological implications, in *Advances in Fission-Track Geochronology*, edited by P. Van den Haute and F. De Corte, pp. 99–112, Springer, New York.

Thiede, R., B. Bookhagen, J. R. Arrowsmith, E. Sobel, and M. Strecker (2004), Climatic control on rapid exhumation along the southern Himalayan Front, *Earth Planet. Sci. Lett.*, *222*, 791–806.

Thiede, R., J. R. Arrowsmith, B. Bookhagen, M. O. McWilliams, E. Sobel, and M. Strecker (2005), From tectonically to erosionally controlled development of the Himalayan orogen, *Geology*, *33*, 689–692, doi:10.1130/G21483.1.

van der Beek, P., B. Champel, and J.-L. Mugnier (2002), Control of detachment dip on drainage development in regions of active fault-propagation folding, *Geology*, *30*, 471–474.

Vannay, J.-C., B. Grasemann, M. Rahn, F. W. A. Carter, V. Baudraz, and M. Cosca (2004), Miocene to Holocene exhumation of metamorphic crustal wedges in the NW Himalaya: Evidence for tectonic extrusion coupled to fluvial erosion, *Tectonics*, *23*, TC1014, doi:10.1029/2002TC001429.

Wang, Q., et al. (2001), Present-day crustal deformation in China constrained by Global Positioning System measurements, *Science*, *294*, 574–577.

Whipp, D. M., Jr., T. A. Ehlers, A. E. Blythe, K. W. Huntington, K. V. Hodges, and D. W. Burbank (2007), Plio-Quaternary exhumation history of the central Nepalese Himalaya: 2. Thermokinematic and thermochronometer age prediction model, *Tectonics*, doi:10.1029/2006TC001991, in press.

Willett, S. D. (1999), Orogeny and orography: The effects of erosion on the structure of mountain belts, *J. Geophys. Res.*, *104*, 28,957–28,981.

Willett, S. D., and M. T. Brandon (2002), On steady states in mountain belts, *Geology*, *30*, 175–178.

Wobus, C. W., K. V. Hodges, and K. X. Whipple (2003), Has focused denudation sustained active thrusting at the Himalayan topographic front?, *Geology*, *31*, 861–864.

Wobus, C. W., A. Heimsath, K. X. Whipple, and K. V. Hodges (2005), Active out-of-sequence thrust faulting in the central Nepalese Himalaya, *Nature*, *434*, 1008–1011.

Zeitler, P. K., N. M. Johnson, C. W. Naeser, and R. A. K. Tahirkheli (1985), Fission-track evidence for Quaternary uplift of the Nanga Parbat region, Pakistan, *Nature*, *298*, 255–257.

A. E. Blythe, Geology Department, Occidental College, 1600 Campus Rd., Los Angeles, CA 90041, USA. (ablythe@oxy.edu)

D. W. Burbank, Department of Earth Science, University of California, Santa Barbara, CA 93106, USA. (burbank@crustal.ucsb.edu)

A. Carter, School of Earth Sciences, Birbeck College, University of London, WC1E 7HX, UK. (a.carter@ucl.ac.uk)

J. Putkonen, Department of Earth and Planetary Science, University of Washington, MS 351310, Seattle, WA 98195-0000, USA. (putkonen@ess.washington.edu)

K. Schmidt, Department of Natural Sciences, Lewis-Clark State College, 500 8th Avenue, Lewiston, ID 83501, USA. (klschmidt@lcsc.edu)